International Journal of Control and Automation
Vol.8, No.10 (2015), pp.361-380
http://dx.doi.org/10.14257/ijca.2015.8.10.33

Algorithm and Accuracy Evaluation of Autonomous Bionic Positioning Method based on Skylight Polarization

Zhen Cheng, Tao Mei, Huawei Liang and Daobin Wang

Department of Automation, University of Science and Technology of China
Hefei Institutes of Physical Science, China Academy of Science
czzb@mail.ustc.edu.cn

Abstract

As the skylight polarization navigation at present is based on dead reckoning which can only provide orientation information to navigate or relative position but not the absolute location of the observer, in this paper, a bionic absolute positioning method based on skylight polarization was proposed: the longitude and latitude of the current position could be solved through the polarization angle of the skylight, the course angle of the vehicle, the relative relationship between the solar and the earth. In addition, the simulation verification provided an accuracy of 0.483km in average. A positioning error model was developed, and the simulation shows that the precision of the sensors has a great impact on the positioning accuracy. Finally, the initial outdoor tests give a longitude accuracy of -0.149° in average and a latitude accuracy of 0.418° in average. Although the positioning accuracy obtained from the experiment is no better than the existing positioning systems, such as GPS, the proposed positioning method which is totally autonomous, convenient and without accumulated error is still worth to be improved since it would be useful when manmade positioning systems are disabled.

Keywords: *skylight polarization navigation; navigation and positioning; bionic positioning; autonomous navigation; celestial navigation*

1. Introduction

With the growing demand for navigation and positioning, satellite navigation systems are in the position of monopoly in the field of navigation and positioning because of their unparalleled precision and speed, especially GPS [1]. However, satellite navigation systems remain powerless under the circumstances of the satellite encrypted or satellite failure, which would result in the losing of navigation information, especially the location of the vehicle. Meanwhile, the commonly used autonomous navigation systems, inertial navigation system (INS) and celestial navigation system (CNS), both have their own disadvantages. The INS couldn't derive the absolute location and would get an accumulated error after used a long time continuously; the CNS is able to derive the absolute location but is complicated, heavy and inefficient within the atmosphere [1]. Therefore, possessing an autonomous absolute positioning capability that does not rely on GPS or other satellite navigation systems is of great importance [2].

Biologists had found that some insects are able to take advantage of the polarized light in the sky to navigate their way home. The bees use some generalized map of the skylight pattern to navigate [3-5]. The neurons of the crickets receive antagonistic input from polarization sensitive photoreceptors with orthogonally arranged analyzer orientations [6]. The desert ant Cataglyphis is able to derive the direction of the nest through the polarized skylight which could be used in path integration to return [7-13]. The beetles were found to consistently orientate along a chosen route usually in the direction of the sun [14]. As one of the autonomous navigation methods commonly used by living creature, the mechanism of the skylight polarization navigation attracts many scientists' attention, and

ISSN: 2005-4297 IJCA

several kinds of bionic polarization navigation sensor and measurement system have been developed. Lambrinos *et al.* [15] developed a typical mobile robot Sahabot 2 which makes use of the pattern of skylight polarization for path-integration and the visual landmark navigation to navigate. Chu *et al. [*16] developed an intelligent mobile robot platform which also takes advantage of the polarization angle for path-navigation to navigate. Wang *et al.* [17] developed an atmospheric polarization measurement system which could measures atmospheric polarization signals with four detecting channels based on time division multiplexing. Qiao [18] developed an atmospheric polarization measurement system which could measure the information of the atmospheric polarization in a region. Yan *et al.* [19] developed a navigation system which can derive a navigation reference line to provide orientation information by building a kind of theoretic and experimental models of the whole polarized sky. However, by reason of the intrinsic property of the polarization navigation sensors that all of them can only derive the orientation with respect to the solar meridian to navigate or relative position combining with other method like dead reckoning, but not the absolute location. Therefore, the skylight polarization navigation right now still cannot replace GPS, or even as an effective supplement once GPS is out of service due to the lack of absolute positioning capability.

In order to find an autonomous positioning method that overcomes the dependency on satellites of GPS, the accumulated error of INS, the inconvenience of CNS, and the lack of absolute positioning capability of present skylight polarization navigation, a bionic positioning method based on skylight polarization and taking advantage of the relative relationship between the solar and the earth was proposed: the current geographic position—latitude and longitude—can be determined by the polarization angle of the skylight, the course angle of the vehicle, the relative relationship between the solar and the earth. The proposed positioning method could be a totally autonomous absolute positioning system independently or a backup positioning system to GPS, INS, and other positioning systems.

2. Mechanism of Polarization Navigation of Desert Ant Cataglyphis

Studies have shown that desert ant Cataglyphis forages for food on a random course which is nearly 200m away from its nest until it finds a suitable prey [7], and the food is carried back on an almost straight line unfailingly just like depicted in Figure 1 [15] below. The reason is that Cataglyphis is able to perceive the symmetrical line of the pattern of the polarized light in the sky due to the response of the polarization-sensitive photoreceptors in the compound eyes. The response signal reaches its extreme value when the body axis of Cataglyphis coincides with the solar meridian. As a result, although Cataglyphis can't derive its current geographic position, it still can accomplish the navigation task by using the direction of skylight polarization as a reference orientation combined with dead reckoning, according to the research of Rossel *et al.* [4], Moller *et al*. [9] and Chu *et al. [*20].

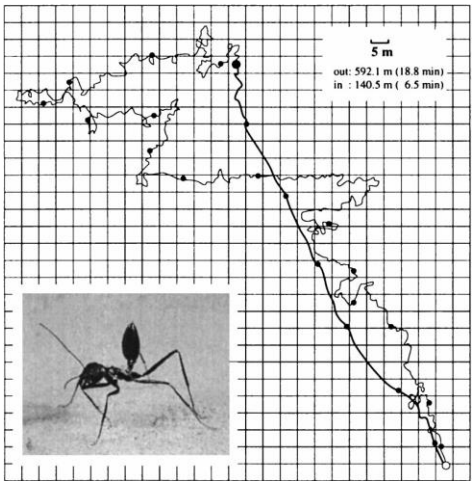

Figure 1. A Typical Foraging Process of Desert Ant Cataglyphis [4]. The Open Circle And Large Filled Circle Represent the Nest and the Position of the Prey Respectively, at the Meantime, the Thin and the Thick Line Represent the Foraging Course and the Heading Home Course, Respectively [15].

It is also shown that the polarization vision of the desert ant Cataglyphis is mediated by a small group of specialized, upward-directed ommatidia situated at the dorsal rim of the compound eye. Each Ommatudium contains two sets of crossed polarization-sensitive photoreceptors. The activity of the polarization-sensitive photoreceptor is a sinusoidal function of e-vector orientation with the maxima and minima separated by 90°, and receive antagonistic input from the polarization-sensitive channels with orthogonal e-vector tuning orientations just like depicted in Figure 2. The crossed-analyzer configuration has the advantage that it enhances e-vector contrast sensitivity and it makes the e-vector response insensitive to fluctuations of light intensity [21].

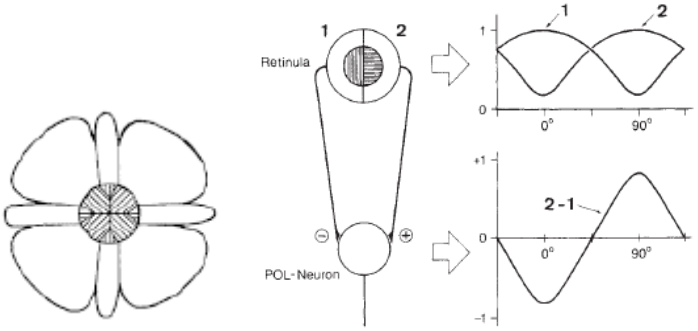

Figure 2. The Polarization Sensitive Part in the Insect Nervous System (Left) and the Principle of Operation of a Polarization-Sensitive Neuron (Right) [15, 24]

Polarization in the sky occurs when the sunlight is scattered by atmosphere molecules [9]. The theoretical patterns of the degree and angle of the polarized light in the sky are calculated by the single-scattering Rayleigh model [21]. According to the single-scattering Rayleigh model, the direction of polarization (e-vector direction) is perpendicular to the plane of scattering determined by the observer, the celestial point observed and the sun in Figure 3.

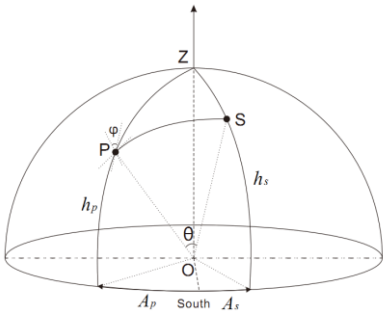

Figure 3. Three-Dimensional Representation of E-Vector Oscillation in The Sky by an Observer in the Centre of the Celestial Hemisphere O, S, P, and Z Represents the Sun, Observation Point in the Celestial Hemisphere, and Zenith Respectively. While H_s, H_p, Θ, A_s, and A_p Represents the Solar Altitude, Altitude of the Observation Point, Solar Azimuth, and Azimuth of the Observation Point Respectively. The Direction of Polarization is Represented by Φ [21]

In the spherical triangle ZPS presented in Figure 3, the law of sine for spherical triangle can be described by the following equation:

$$\frac{\sin \angle ZPS}{\sin\left(90°\text{-}h_s\right)} = \frac{\sin\left(A_s - A_p\right)}{\sin\theta}$$

That is,

$$\cos\varphi = \frac{\sin\left(A_s - A_p\right)}{\sin\theta} \times \cos h_s \tag{1}$$

Meanwhile, the degree of the skylight polarization P can be described by:

$$P(\theta) = \frac{1\text{-}\cos^2\theta}{1+\cos^2\theta} \cdot P_{max} = \frac{\sin^2\theta}{1+\cos^2\theta} \cdot P_{max} \tag{2}$$

Where Pmax represents the maximum value of P.

Therefore, the value of φ which represents the direction of polarization and P, describe the skylight polarization of a single point P, can be calculated by Equation (1) and Equation (2) above. And the Cataglyphis do make use of the direction of skylight polarization φ as a reference orientation combined with dead reckoning to navigate exactly.

However, when considering the polarization of the whole sky not only a single point P, the situation of the full skylight polarization can be described as the pattern of skylight polarization just like depicted in Figure 4.

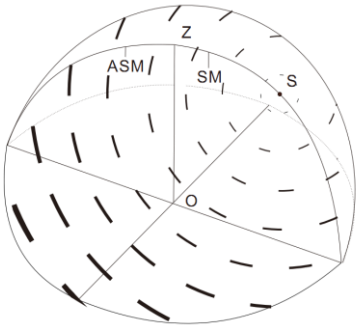

Figure 4. Three-Dimensional Representation of the Pattern of the Polarized Light in the Sky by an Observer in the Centre of the Celestial Denoting by O, the Direction and Degree of Polarization is Depicted by the Orientation and the Width of the Black Bar, the Pattern is Bilateral Symmetry by a Line Named the Solar Meridian (SM) which is Running Through the Sun (S) and Zenith (Z), and the Anti-Solar Meridian (ASM) on the Opposite Side [12, 19, 21].

In addition, the pattern of skylight polarization is relatively stable as long as the time and position of the observer is settled according to Equation (1) and Equation (2) [20] [22].

According to the mechanisms of the polarization-sensitive neurons of desert ant Cataglyphis and the pattern of skylight polarization, the bionic polarization navigation sensor is developed to derive the orientation with respect to the solar meridian directly [19, 22].

3. Bionic Positioning Algorithm

Inspired by the mechanisms of the polarization-sensitive neurons and the navigation strategy implemented by desert ant Cataglyphis, which make use of the direction of skylight polarization as a reference orientation in dead reckoning to navigate but having the disadvantage of cannot derive the absolute location, the bionic positioning method by taking advantage of the skylight polarization angle but abandoning dead reckoning is proposed. The latitude and longitude can be determined by course angle, the orientation with respect to the solar meridian, and the relative position between the solar and the earth.

3.1. Positioning Procedure

The procedure of the bionic positioning algorithm based on skylight polarization navigation is shown in Figure 5. First of all, the course angle α_0 is measured by high precision electronic compass. Secondly, the direction of polarization β_1 and β_2 is detected by polarization angle sensor at the moment T_1 and T_2 respectively. Thirdly, the solar declination δ_1 and δ_2 at the moment T_1 and T_2, and the equation of time t_0, which describes the difference between apparent solar time and mean solar time, is obtained by inquiring the ephemeris. Finally, the latitude and longitude of the observer can be worked out based on the navigation triangle in celestial navigation.

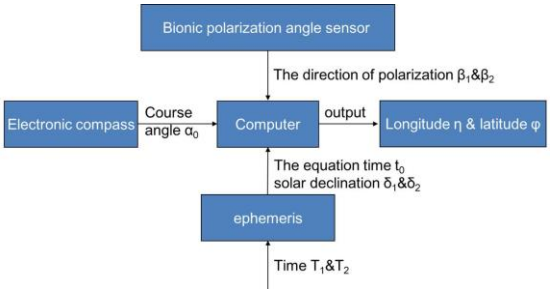

Figure 5. Description of the Procedure of the Bionic Positioning Algorithm

3.2. Navigation Triangle

In celestial navigation, the altitude and azimuth of the celestial body can be derived by solving the navigation triangle with the right ascension and declination looked up in the ephemeris and the projection of the celestial body on the earth [2]. However, the navigation triangle in Figure 6 clearly reveals the relative relationship of the sun, the earth and the observer, which can be used to calculate the longitude and latitude of the observer together with the skylight polarization angle.

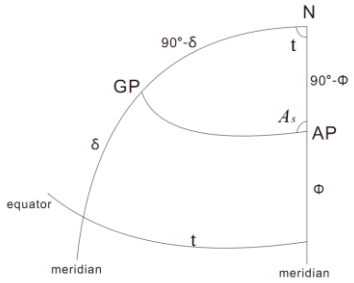

Figure 6. Description of the Navigation Triangle in Celestial Navigation. GP, AP, A_s, T, Δ And Φ Represents the Projection of the Sun on the Earth, the Position of the Observer, the Solar Azimuth, the Solar Hour Angle, the Solar Declination, and the Latitude of the Observer Respectively. While the Solar Hour Angle is an Angle Measured from the Meridian of the Observer to the Meridian of the Sun along the Celestial Equator [23]

The solar altitude h can be described by the following equation:

$$\sin h = \sin\phi \sin\delta + \cos\phi \cos\delta \cos t \tag{3}$$

While the solar azimuth A_s can be described by:

$$\cos A_s = \frac{\sin h \sin\phi - \sin\delta}{\cos h \cos\phi} \tag{4}$$

Equation (3) and Equation (4) above describes the relative relationship between the solar, the earth and the observer. Therefore, once A_s, h, δ is known, the latitude of AP ϕ and the solar hour angle t which is used to determine the longitude of AP with the solar ascension, can be solved by Equation (3) and Equation (4) above.

3.3. Algorithm Derivation

With the navigation triangle above, the geographic position of observer Z at a certain moment coincides with the equations below:

$$\sin h_s = \sin\phi \sin\delta + \cos\phi \cos\delta \cos t \tag{5}$$

$$\cos A_s = \frac{\sin h_s \sin\phi - \sin\delta}{\cos h_s \cos\phi} \tag{6}$$

The latitude ϕ and the solar hour angle t are parameters to be determined in Equation (5) and Equation (6).

Meanwhile, submitting $A_p=\alpha_0$ and $\varphi=\beta-\pi/2$ into Equation (1), where β and α_0 represents skylight polarization angle and the course angle, respectively. Equation (1) then becomes like this:

$$\cos(\beta - \pi/2) = \frac{\sin(A_s - \alpha_0)}{\sin\theta}$$

Furthermore, $\theta=\pi/2-h_s$ is submitted into the equation above when the observation point P moves to zenith Z, we could have:

$$\cos\varphi = \sin(A_s - \alpha_0)$$

That is,

$$A_s = \pi - (\beta - \alpha_0) \tag{7}$$

The solar declination δ can be obtained through ephemeris, while the solar azimuth A_s can be determined by Equation (7) since β and α can be measured. However, in order to determine ϕ and t, there is still an unknown parameter h_s. Therefore, ϕ and t which are used to determine the latitude and longitude of the observer cannot be calculated by one single measurement.

Whereas, considering the direction of polarization β_1 and β_2 detected by polarization angle sensor at the moment T_1 and T_2, there are 4 linearly independent equations with 5 unknown parameters: ϕ, h_{s1}, h_{s2}, t_1 and t_2, which cannot be worked out apparently. While with Equation (8) below, there comes 4 unknown parameters with 4 linearly independent equations, ϕ and t_1 can be calculated accordingly.

$$t_2 = t_1 + (T_2 - T_1) * 15° * 2\pi / 360° = t_1 + \Delta \tag{8}$$

First, Equation (6) then becomes:

$$\cos^2 A_s \cos^2 h_s \cos^2\phi = \sin^2 h_s \sin^2\phi + \sin^2\delta - 2\sin h_s \sin\delta \sin\phi \tag{9}$$

Then,

$$\sin^2 h_s = (\sin\phi \sin\delta + \cos\phi \cos\delta \cos t)^2 \tag{10}$$

Substituting Equation (10) into Equation (5):

$$\begin{aligned}&(\sin^2 A_s \cos^2\delta \cos^4\phi - \cos^2\delta \cos^2\phi)\cos^2 t + \sin^2 A_s \sin 2\delta \sin\phi \cos^3\phi \cos t \\ &- \sin^2 A_s \sin^2\delta \cos^4\phi + \cos^2 A_s \cos^2\delta \cos^2\phi = 0\end{aligned} \tag{11}$$

That is,

$$a(\phi)\cos^2 t+b(\phi)\cos t+c(\phi)=0 \tag{12}$$

Where,

$$a(\phi)=\sin^2 A_s \cos^2\delta\cos^4\phi-\cos^2\delta\cos^2\phi \tag{12a}$$

$$b(\phi)=\sin^2 A_s \sin 2\delta\sin\phi\cos^3\phi \tag{12b}$$

$$c(\phi)=-\sin^2 A_s \sin^2\delta\cos^4\phi+\cos^2 A_s \cos^2\delta\cos^2\phi \tag{12c}$$

And $a(\phi)$, $b(\phi)$, $c(\phi)$ are all single-valued function of ϕ.

From the equations above, at the moment T_1 and T_2, there are:

$$\begin{cases} a_1(\phi)\cos^2 t_1+b_1(\phi)\cos t_1+c_1(\phi)=0 \\ a_2(\phi)\cos^2 t_2+b_2(\phi)\cos t_2+c_2(\phi)=0 \end{cases} \tag{13}$$

The latitude of the observer ϕ and t_1 can be calculated by Equation (13) finally.

In addition, the apparent solar time tapparent of the observer at the moment T_1 can be determined as followed:

$$\begin{cases} t_{apparent} = t_1/15+12 & \text{morning} \\ t_{apparent} = t_1/15 & \text{afternoon} \end{cases} \tag{14}$$

Combined with the equation time t_0 looked up in the ephemeris, the mean solar time tmean at the moment T_1 can be described by the relationship $t_{mean}=t_{apparent}-t_0$. Therefore, the longitude of the observer η is determined by the equation:

$$\eta=(t_{mean}-T_1)*15° \tag{15}$$

Where the time system of T_1 is universal time.

4. Simulation Verification

Just like presented in Figure 5, the current geographic position can be calculated as long as β_1, β_2, α_0 are measured by the sensors, and δ_1, δ_2, t_0 are obtained in the ephemeris by the bionic positioning algorithm. Because of the solar azimuth A_s has a linear relationship with β and α_0 due to Equation (7), and As is available in the ephemeris as well as δ_1, δ_2 and t_0, the ephemeris provided by Purple Mountain Observatory of the Chinese Academy of Science (PMO） is used to do some verification and accuracy evaluation firstly.

However, the data provided by the PMO is measured by TT time system, while the bionic positioning algorithm proposed is based on UTC time system. Therefore, the transformation between different time systems should be added into the bionic positioning system to unify the time system.

The relationship between them is presented below:

$$UTC=UT-\Delta UT=(TT-\Delta T)-\Delta UT \tag{16}$$

In a short period of time, the relationship can be described as following:

$$UTC = \left(TT - 32.184s - \left(TAI - UTC\right) + \left(UT - UTC\right)\right) - \Delta UT$$
$$= TT - 32.184s - \left(TAI - UTC\right) \tag{17}$$

where *UTC*, *UT*, *ΔUT*, *TT*, *TAI* represents the UTC time system, UT time system, the difference of UT and UTC, TT time system, and TAI time system respectively, while the value of *TAI-UTC* can be obtained from the website of the Earth Orientation Center.

According to the ephemeris provided by PMO, the equation of time t0=3′39.9″, and data of a full trajectory on 16th May 2013, in Beijing (39°54'N, 116°46'E) was derived.

The positioning result is presented in Figure 7, comparing with the actual latitude and longitude of observation (39.900000°N, 116.766667°E), the latitude error is -0.051′ in average, the longitude error is 0.264′ in average, and the distance error is 0.483km in average, which consistent with the actual value basically. Therefore, the bionic positioning method is proved feasible.

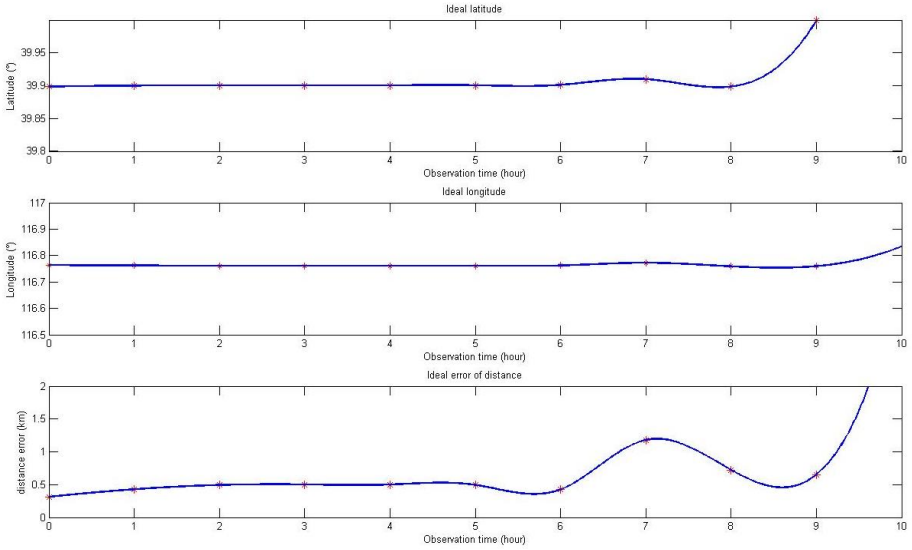

Figure 7. Simulation Result of the Bionic Positioning Algorithm at the Position 39.900000°N, 116.766667°E on 16th May 2013, where Blue Line Represents the Position Calculated by the Bionic Positioning Algorithm and the Red * Represents the Actual Position of the Vehicle at the Scattered Observation Time (Horizontal Axis)

5. Positioning Error Model

In order to do error analysis and accuracy evaluation, the positioning error model has been developed as follows.

First of all, the longitudinal error and lateral error has the relationship as below

$$\begin{cases} \delta_y = R_E \delta_\phi \\ \delta_x = R_E \phi \delta_\eta \end{cases} \tag{18}$$

Where RE represents the radius of the earth, δ_ϕ, δ_η represents the positioning error in the form of latitude and longitude, and δ_x, δ_y represents the lateral error and vertical error.

Meanwhile,

$$\begin{cases} \delta_{\phi}=\sqrt{\left(\dfrac{\partial\phi}{\partial A_{s1}}\right)^2 \delta_{A_{s1}}{}^2+\left(\dfrac{\partial\phi}{\partial A_{s2}}\right)^2 \delta_{A_{s2}}{}^2+\left(\dfrac{\partial\phi}{\partial\delta_1}\right)^2 \delta_{\delta_1}{}^2+\left(\dfrac{\partial\phi}{\partial\delta_2}\right)^2 \delta_{\delta_2}{}^2} \\ \delta_{\eta}=\sqrt{\left(\dfrac{\partial\eta}{\partial A_{s1}}\right)^2 \delta_{A_{s1}}{}^2+\left(\dfrac{\partial\eta}{\partial A_{s2}}\right)^2 \delta_{A_{s2}}{}^2+\left(\dfrac{\partial\eta}{\partial\delta_1}\right)^2 \delta_{\delta_1}{}^2+\left(\dfrac{\partial\eta}{\partial\delta_2}\right)^2 \delta_{\delta_2}{}^2} \end{cases} \tag{19}$$

Where δ_{As1}, δ_{As2} represents the error of A_s of the first and second observation, while $\delta_{\delta 1}$, $\delta_{\delta 2}$ represents the error of δ of the first and second observation.

According to Equation (14) and Equation (15), there comes

$$\eta=\begin{cases} \left(t_1/15+12-t_0-T_1\right)\times 15°\text{morning} \\ \left(t_1/15-t_0-T_1\right)\times 15°\text{afternoon} \end{cases} \tag{20}$$

Thus,

$$\delta_{\eta}=\delta_{t_1} \tag{21}$$

Where δ_{t1} represents the error of t_1.

And

$$\delta_r=\sqrt{\left(\delta_x\right)^2+\left(\delta_y\right)^2} \tag{22}$$

Where δ_r represents the distance error.

When the left side of Equation (13) is written as F_1 and F_2, then Equation (13) becomes like this,

$$\begin{cases} F_1=a_1(\phi)\cos^2 t_1+b_1(\phi)\cos t_1+c_1(\phi) \\ F_2=a_2(\phi)\cos^2 t_2+b_2(\phi)\cos t_2+c_2(\phi) \end{cases} \tag{23}$$

Due to the explicit solution of Equation (13) provided by the bionic positioning method could not be found, the partial derivatives can be worked out by Equation (24) below.

$$\begin{cases} \frac{\partial F_1}{\partial A_{s1}}+\frac{\partial F_1}{\partial \varphi}\frac{\partial \phi}{\partial A_{s1}}+\frac{\partial F_1}{\partial t_1}\frac{\partial t_1}{\partial A_{s1}}=0 \\ \frac{\partial F_2}{\partial A_{s1}}+\frac{\partial F_2}{\partial \varphi}\frac{\partial \phi}{\partial A_{s1}}+\frac{\partial F_2}{\partial t_1}\frac{\partial t_1}{\partial A_{s1}}=0 \\ \frac{\partial F_1}{\partial A_{s2}}+\frac{\partial F_1}{\partial \varphi}\frac{\partial \phi}{\partial A_{s2}}+\frac{\partial F_1}{\partial t_1}\frac{\partial t_1}{\partial A_{s2}}=0 \\ \frac{\partial F_2}{\partial A_{s2}}+\frac{\partial F_2}{\partial \varphi}\frac{\partial \phi}{\partial A_{s2}}+\frac{\partial F_2}{\partial t_1}\frac{\partial t_1}{\partial A_{s2}}=0 \\ \frac{\partial F_1}{\partial \delta_1}+\frac{\partial F_1}{\partial \varphi}\frac{\partial \phi}{\partial \delta_1}+\frac{\partial F_1}{\partial t_1}\frac{\partial t_1}{\partial \delta_1}=0 \\ \frac{\partial F_2}{\partial \delta_1}+\frac{\partial F_2}{\partial \varphi}\frac{\partial \phi}{\partial \delta_1}+\frac{\partial F_2}{\partial t_1}\frac{\partial t_1}{\partial \delta_1}=0 \\ \frac{\partial F_1}{\partial \delta_2}+\frac{\partial F_1}{\partial \varphi}\frac{\partial \phi}{\partial \delta_2}+\frac{\partial F_1}{\partial t_1}\frac{\partial t_1}{\partial \delta_2}=0 \\ \frac{\partial F_2}{\partial \delta_2}+\frac{\partial F_2}{\partial \varphi}\frac{\partial \phi}{\partial \delta_2}+\frac{\partial F_2}{\partial t_1}\frac{\partial t_1}{\partial \delta_2}=0 \end{cases} \tag{24}$$

Finally, the positioning error model can be settled by the solving Equation (24), that is,

$$\begin{cases} \delta_\phi = f\left(A_{s1},\delta_1,A_{s2},\delta_2,\phi,t_1,d,\delta_{A_{s1}},\delta_{A_{s2}},\ \delta_{\delta_1},\delta_{\delta_2}\right) \\ \delta_\eta = f\left(A_{s1},\delta_1,A_{s2},\delta_2,\phi,t_1,d,\delta_{A_{s1}},\delta_{A_{s2}},\delta_{\delta_1},\delta_{\delta_2}\right) \end{cases} \tag{25}$$

Where d represents the difference of T_1 and T_2.

6. Accuracy Evaluation

6.1. The Impact of Precision of the Sensors on Positioning Accuracy

Precision of the sensor has an impact on the positioning accuracy obviously. To find out the relationship between the positioning accuracy and the precision of electronic compass and polarization angle sensor, some simulations were carried out. Then Equation (25) becomes

$$\begin{cases} \delta_\phi = f\left(A_{s1},\delta_1,A_{s2},\delta_2,\phi,t_1,d,\delta_{A_{s1}},\delta_{A_{s2}}\right) \\ \delta_\eta = f\left(A_{s1},\delta_1,A_{s2},\delta_2,\phi,t_1,d,\delta_{A_{s1}},\delta_{A_{s2}}\right) \end{cases} \tag{26}$$

Because of the solar azimuth A_s has a linear relationship with β and α_0 due to Equation (7), the error of the sensors also have a linear impact on A_s. Besides, A_s is available in the ephemeris provided by PMO as well as δ_1, δ_2 and t_0, wherefore the accuracy evaluation on the impact of precision of the sensors on positioning accuracy was carried out in the form of solar azimuth A_s in the first place, and the result is presented in Figure 8 and Figure 9. Comparing with the actual latitude and longitude of observation (39.900000°N, 116.766667°E), the positioning error was proportional with the sensor error when the error of the sensor was no more than 1′ and 1″. The latitude error was 0.6°, longitude error was 0.5°, and distance error was 76km when the sensor error was 1′, while the latitude

error was 0.009°, longitude error was 0.008°, and distance error was 1.27km when the sensor error was 1″. The result demonstrates that the positioning accuracy is linearly stable with the sensor error.

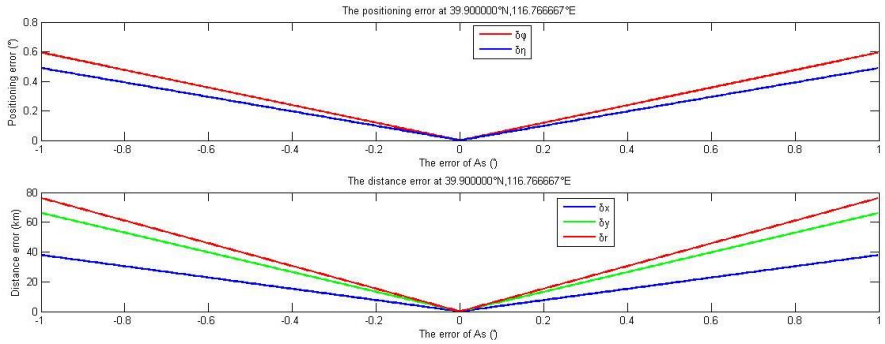

Figure 8. The Impact of Precision of the Sensors on Positioning Accuracy of the Bionic Positioning Algorithm when the Sensor Error is 1′ at the Position 116.766667°E, 39.900000°N on 16th May 2013, where Δ_ϕ, Δ_η Represents the Positioning Error in the Form of Latitude and Longitude, while Δ_x, Δ_y, Δ_r Represents the Lateral Error, Vertical Error, and Distance Error Respectively

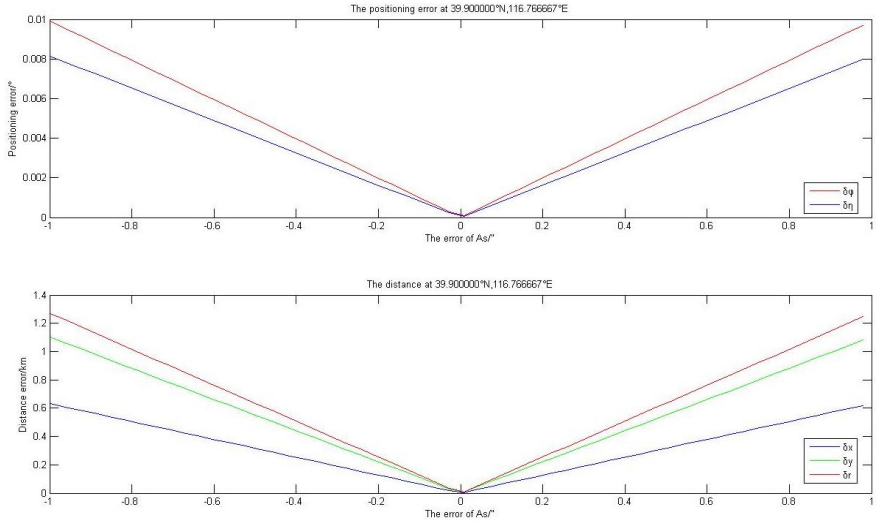

Figure 9. The Impact of Precision of the Sensors on Positioning Accuracy of the Bionic Positioning Algorithm when the Sensor Error Is 1″ at the Position 116.766667°E, 39.900000°N on 16th May 2013, where Δ_ϕ, Δ_η Represents the Positioning Error in the Form of Latitude and Longitude, while Δ_x, Δ_y, Δ_r Represents the Lateral Error, Vertical Error, and Distance Error Respectively

6.2. The Impact of the Accuracy of Solar Declination Δ On Positioning Accuracy

To evaluate the impact of the accuracy of solar declination δ on positioning accuracy, Equation (25) becomes

$$\begin{cases} \delta_{\phi}=f\left(A_{s1},\delta_1,A_{s2},\delta_2,\phi,t_1,d,\delta_{\delta_1},\delta_{\delta_2}\right) \\ \delta_{\eta}=f\left(A_{s1},\delta_1,A_{s2},\delta_2,\phi,t_1,d,\delta_{\delta_1},\delta_{\delta_2}\right) \end{cases} \tag{27}$$

Some evaluation experiments were carried out and the result is presented in Figure 10.

Because the solar declination δ is stable and has a small fluctuation under 1°*10-5, the evaluation was carried out when the error of δ is between -1°*10-5 to 1°*10-5. Comparing with the actual latitude and longitude of observation (39.900000°N, 116.766667°E), the latitude error was proportional with the error of solar declination δ when the error of δ is -1°*10-5~1°*10-5, while the latitude error was 0.005°, longitude error was 0.004°, and distance error was 0.34km. That means the accuracy of the solar declination δ has a slight impact on the positioning accuracy and stability of the bionic positioning method as the solar declination error is between -1°*10-5 to 1°*10-5.

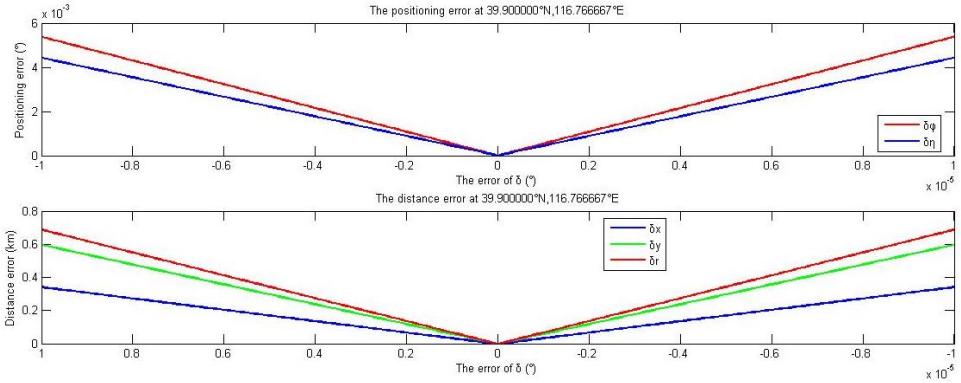

Figure 10. The Impact of the Accuracy of Solar Declination *Δ* on Positioning Accuracy of the Bionic Positioning Algorithm at the Position 116.766667°E, 39.900000°N on 16th May 2013, where Δ_{ϕ}, Δ_{η} Represents the Positioning Error in the Form of Latitude and Longitude, while Δ_x, Δ_y, Δ_r Represents the Lateral Error, Vertical Error, and Distance Error Respectively.

6.3. The Impact of the Location of Observer on Positioning Accuracy

To discuss the application range, the impact of the location of the observation, especially latitude, on positioning accuracy is observed through some simulations as below. A set of full trajectory data at 120°E, from 10°N to 80°N on 16th May 2013 was obtained.

The data processing result is presented in Figure 11, comparing with the actual latitude and longitude of the observer (120°E, 10°N~80°N), the latitude error is between -1.76975′~1.554779′, and the longitude error is between -0.473172′~0.884443′, and the distance error in average is between 0.482723km~1.82995km. Meanwhile, the average distance error reached its maximum value—1.82995km at 20°N, 120°E, and the average distance error was below 1km between 30°N, 120°E to 70°N, 120°E. On the other hand, the invalid observation reached its max at 10°N, 120°E. That demonstrates the positioning accuracy and stability is higher between the latitude 30°N~70°N than at low latitude or high latitude, which means that the application range of the bionic positioning method is at middle latitude while the longitude is not limited.

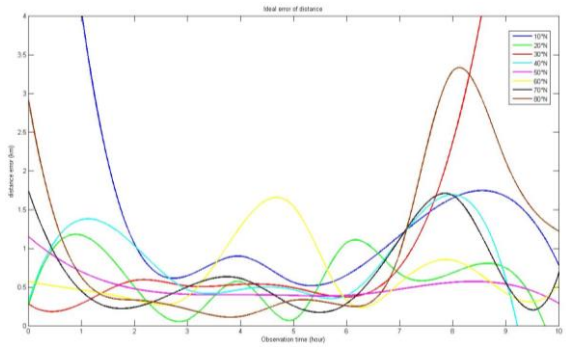

Figure 11. Ideal Result of the Bionic Positioning Algorithm at the Position 120°E, 10°N~80°N on 16th May 2013, where Lines Represent the Position Error Calculated by the Bionic Positioning Algorithm And * Represents the Actual Position Error of the Vehicle at the Scattered Observation Time (Horizontal Axis)

7. Experiment

7.1. The Structure of the Bionic Positioning System

Although some simulation test have been carried out in section 4, and results preliminary verified the feasibility of the method, a bionic skylight polarization positioning system has been built to implement outdoor tests.

The hardware of the bionic skylight polarization positioning system fixed on a vehicle consists of a three-camera skylight polarization angle measuring module, a course angle module and a computer processing module as shown in Figure 12. The upper part is the three-camera skylight polarization angle measuring module, in which the linear polarization filter over the camera is located as 0°, 45° and 90°. The lower part is the course angle measuring module, which make use of an OCTANS INS to provide the course angle of the vehicle. The computer processing module does not appear in Figure 12. The positioning system is assembled to make sure that the 0° direction of the OCTANS INS is always consistent with the 0° channel camera as the 0° direction of the positioning system.

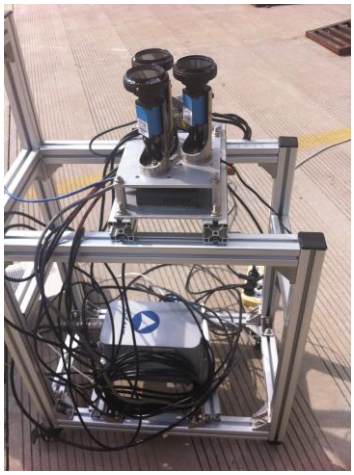

Figure 12. Experimental Platform of the Bionic Positioning Method Based on Skylight Polarization

As the core of the bionic skylight polarization positioning system which is shown in Figure 13, the three-camera skylight polarization angle measuring module consists of three groups of measuring units with the same structure. In each measuring unit, the skylight through a blue filter and a linear polarizer reaches the camera, the intensity information of the polarized skylight captured by the camera is sent into the computer for further processing. The three measuring units are located as 0°, 45° and 90° due to the linear polarizer over the camera. The polarization angle β of the skylight could be solved through the calculation of the Stocks vector. The direction information, which actually is the course angle α_0 of the vehicle, is provided by the OCTANS INS. The longitude and latitude of the vehicle could be calculated as long as β_1, β_2, α_0 are measured by the sensors, and δ_1, δ_2, t_0 are obtained in the ephemeris by the bionic positioning algorithm.

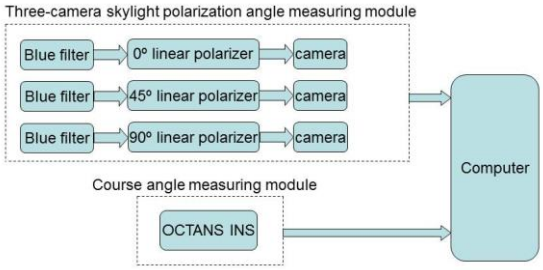

Figure 13. Hardware Structure of the Bionic Position System

7.2. Experiment Result

As the three-camera skylight polarization angle measuring module is affected by the pattern of skylight polarization , in order to achieve better results, the experiment is carried out in the morning of 14th March 2014, sunny, and the location of the vehicle is 31.850130°N, 117.129117°E. In the whole experimental procedure, the vehicle receives the skylight without any block neither by buildings nor shadows.

In the outdoor test, the location of the vehicle remains unchanged on 31.850130°N, 117.129117°E, while the course angle after maintained at 13.25° for a period of time, changed to 57.84° for another period of time by turning the vehicle. Therefore, the continuous acquisition of the polarization angle of the vehicle carried out under the circumstance of same location but different course angle. Thus, the corresponding longitude and latitude curve and error curve is draw according to the data of the experiment.

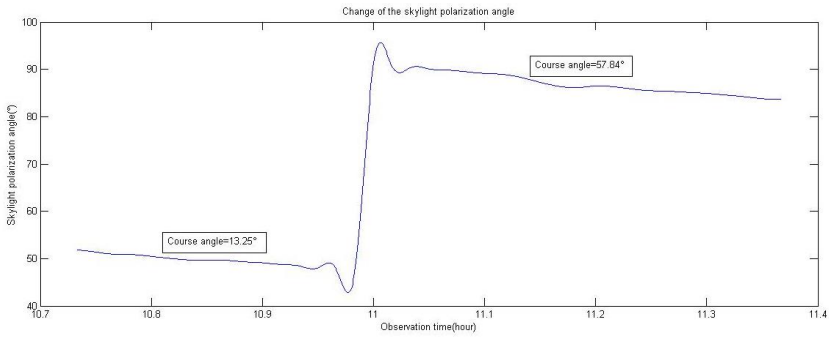

Figure 14. The Change of the Polarization Angle of the Skylight

Figure 14 shows the polarization angle curve received by the three-camera skylight polarization angle measuring module from 10:50am to 11:22am. The curve can be divided into 2 parts, the first part keeps the course angle of 13.25° with the polarization

angle changing from 51.798° to 47.511° slowly, and the course angle of the second part is 57.84° with the polarization angle changing from 91.017° to 83.693° after a jump of 43.506° from 47.511° to 91.017°. Obviously, the 43.506°'s jump of the polarization angle dues to the 44.59°'s jump of the course angle from 13.25° to 57.84°, which means the polarization angle is stable in a period of time at the same location, and the polarization angle changes with the change of the course angle because of both of them take 0° of the vehicle as the direction reference.

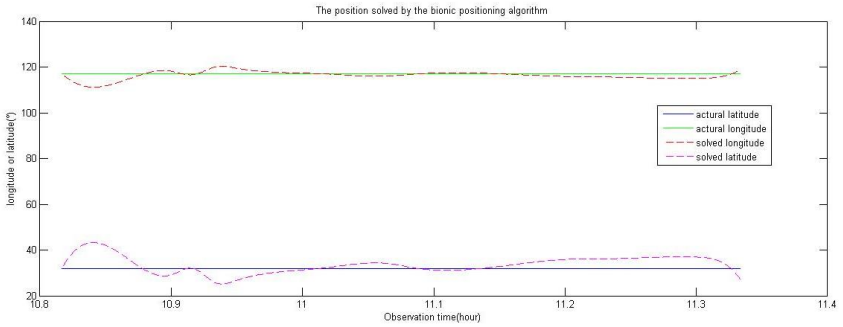

Figure 15. The Position Solved by the Bionic Positioning Method

According to the polarization angle derived with the corresponding course angle, the curve of the longitude and latitude of the vehicle is showed in Figure 15. The calculated latitude and longitude is coincide with the actual position basically within the half an hour's continuous observation. Besides, as long as the location of the vehicle and the course angle remains unchanged between the two observations which is a requirement for positioning, the positioning accuracy of the bionic positioning algorithm is not affected, whether the course angle of the vehicle changes or not. Furthermore, because of the inherent advantage of the positioning method, the method does not have the problem of accumulated error, and the experiment results are relatively stable. The result of outdoor test shows that the bionic positioning method is feasible.

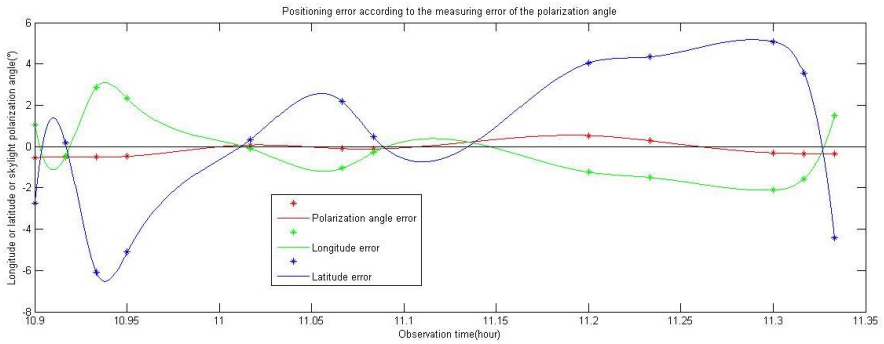

Figure 16. The Positioning Error According to the Change of Measuring Error of Polarization Angle

As demonstrated in the positioning error model, the precision of the sensor has a great impact on positioning accuracy, thus the positioning error which changes in the curve with the measuring error of polarization angle is shown in Figure 16. Longitude error and latitude error shows a significant positive correlation, the frequency and amplitude of the two curves are almost strictly synchronous with time, although in the opposite direction. Moreover, the positioning error shows a significant positive correlation with the measuring error of polarization angle. Furthermore, the longitude accuracy is -0.149° in average, while the latitude accuracy is 0.418° in average, which coincides with the

positioning error model basically although the error is not small compared to other positioning systems. Therefore, the key to improve the positioning accuracy is to reduce the measuring error of polarization angle.

8. Conclusion

In this paper, a bionic positioning method based on skylight polarization sensor was proposed to measure the latitude and longitude of the current position by two independent observations of the polarized skylight. The current absolute location, latitude and longitude, can be determined by the bionic positioning algorithm when the course angle α_0 is measured by electronic compass, the equation of the time t_0 is looked up in the ephemeris, the orientation with respect to the solar meridian β_1 and β_2 is detected by polarization angle sensor, and the solar declination δ_1 and δ_2 is looked up in the ephemeris at the moment T_1 and T_2 respectively. The simulation result demonstrates that the positioning accuracy of the autonomous bionic positioning method is 0.485km in average. The impact factors that affect positioning accuracy have been analyzed, including the precision of the sensors, the accuracy of solar declination δ, and the location of the observer. The precision of the sensors has a great impact on positioning accuracy while solar declination δ and equation time t_0 has a slight impact. Besides, the suitable application range of the positioning method is at middle latitude while the longitude is not limited. Moreover, a bionic positioning system consists of a three-camera skylight polarization angle measuring module, a course angle measuring module and a computer processing module is presented. The initial experiment results of the outdoor tests give an average positioning accuracy of -0.149° in longitude and 0.418° in latitude. Although the positioning accuracy obtained from the simulation and the experiment is no better than the existing positioning systems, such as GPS, the proposed positioning method overcomes the disadvantage of INS, CNS, and the present skylight polarization navigation system. It provides an alternative way to derive the longitude and latitude when manmade positioning systems are disabled.

Since the positioning accuracy has to be improved, our future work will focus on how to improve measuring accuracy of the skylight polarization angle measuring module and develop an error compensation algorithm.

Acknowledgements

The authors would like to express our gratitude to the financial supports from National Basic Research Program of China (973 Program) under Grant No. 2011CB302100, the National Natural Science Foundation of China under Grant No. 91120307 and the National Natural Science Foundation of Chine under Grant No. 91320301.

References

[1] S.F. Bian and W.K. Li, "Introduction to satellite navigation system, Publishing House of Electronics Industry", Beijing, China, **(2005),** pp.1-8.
[2] Z. Cheng, T. Mei and H.W. Liang, "Positioning algorithm based on skylight polarization navigation", Proceeding of 8th IFAC Symposium on Intelligent Autonomous Vehicles, **(2013)** June 26-28; Gold Coast, Australia, Vol.8, No.1, 97-101.
[3] S. Rossel and R. Wehner, "The bee's map of the e-vector pattern in the sky", Proc. Natl. Acad. Sci. USA, Neurobiology. 79 **(1982).**
[4] S.Rossel and R. Wehner, "How bees analyze the polarization patterns in the sky", Journal of Comparative Physiology A. 154 **(1984)**
[5] S. Rossel and R. Wehner, "Polarization vision in bees", Nature. 323 **(1986)**
[6] T. Labhart, "Polarization-opponent interneurons in the insect visual system", Nature. 331 **(1988).**
[7] R. Wehner, "Spatial organization of foraging behaviour in individually searching desert ants, Cataglyphis (Sahara desert) and Ocymyrmes (Namib desert)", Individual to Collective Behavior in Social Insects, **(1987)** Birkhauser, Basel, 15-42.

[8] G. Hartmann and R. Wehner, "The ant's path integration system: a neural architecture", Biological Cybernetics. 73 **(1995)**
[9] R. Moller, D. Lambrinos, R. Pfeifer, T. Labhart and R. Wehner, "Modeling Ant Navigation with an Autonomous Agent. Proc. SAB (**1998)**
[10] E. P. Meyer and V. Domanico, "Microvillar orientation in the photoreceptors of the ant Cataglyphis bicolor", Cell Tissue Res. 295 **(1999).**
[11] M. Collett and T. S. Collett, "How do insects use path integration for their navigation? Biological Cybernetics", 83 **(2000).**
[12] R. Wehner, "Desert ant navigation: how miniature brains solve complex tasks", Journal of Comparative Physiology A. 189 **(2003).**
[13] M. Sakura, D. Lambrinos and T. Labhart, "Polarized Skylight Navigation in insects: Model and Electrophysiology of e-vector Coding by Neurons in the Central Complex", Journal of Neurophysiology, 99 **(2008).**
[14] M. Byrne, M. Dacke, P. Nordstrom, C. Scholtz and E. Warrant, "Visual cues used by ball-rolling dung beetles for orientation", Journal of Comparative Physiology A, 189 **(2003).**
[15] D. Lambrinos, R. Moller, T. Labhart, R. Pfeifer and R. Wehner, "A mobile robot employing insert strategies for navigation. Robotics and Autonomous Systems", 30 **(2000).**
[16] R.H. Li, J.K. Chu, C.L. Xu and Q.Y. Li, "Design and realization of intelligent mobile robot platform for micro navigation sensors", Transducer and Microsystem Technologies, vol.27, No.10 **(2008).**
[17] X.F. Huang, Y. Bu and X.C. Wang, "Four-Channel Division Multiplexing Atmospheric Polarization Measurement technique Based on Vision Bionics", Chinese Journal of Lasers, vol. 47, No. 8 **(2010).**
[18] X.B. Sun, J. Hong and Y.L. Qiao, "Investigation of measurements of polarized properties of atmospheric scattering radiation", Chinese journal of quantum electronics, vol.22, No. 1 **(2005).**
[19] L. Yan, G. X. Guan, J.B. Chen, T.X. Wu and X. Shao, "The Bionic Orientation Mechanism in the Skylight Polarization Pattern", Acta Scientiarum Universitatis Pekinnensis, vol.45, No.4 **(2009).**
[20] J.K. Chu and K.C. Zhao, "Study of Angle Measurement Optoelectronic Model on Emulating Polarization-Sensitive Compound Eye of Insect", Nanoelectronic Device & Technology, 12 **(2005).**
[21] J.K. Chu, K.C. Zhao, Q.Zhang and T. Wang, "Construction and performance test of novel polarization sensor for navigation' Sensor and Actuators A, 148 **(2008).**
[22] [22] G. X. Guan, L. Yan, J.B. Chen and T.X.Wu. "Dynamic Property of Skylight Polarization pattern Graph", Computer Applications and Software, vol.12, No.12 **(2009).**
[23] J.C. Fang and X.L. Ning, "Principle and Application of celestial navigation, 2nd ed.", Beijing University of Aeronautics and Astronautics Press, Beijing, China **(2006).**
[24] T. Labhart and E.P. Meyer, "Detectors for polarized skylight in insects: a survey of ommatidial specializations in the dorsal rim area of the compound eye", Microscopy research and technique, vol.47, No.6 **(1999).**

Authors

Cheng Zhen, she was born in Jiangxi, China. She is a doctoral student in University of Science and Technology of China. Her interests include Navigation, bionic positioning and autonomous localization.

Tao Mei, he is a professor in University of Science and Technology of China, and Hefei Institutes of Physical Science, China Academy of Science. His interests include robotics, navigation and positioning, and intelligent vehicle.

Huawei Liang, he is a professor in Hefei Institutes of Physical Science, China Academy of Science. His interests include navigation and positioning, intelligent vehicle, skylight polarization navigation.

Daobin Wang, he is a doctoral student in University of Science and Technology of China. His interests include skylight polarization navigation, SLAM, and signal processing.